JOC The Journal of Organic Chemistry

Article

pubs.acs.org/joc

Strategically Modified Rhodamine–Quinoline Conjugate as a CHEF-Assisted FRET Probe for Au^{3+}: DFT and Living Cell Imaging Studies

Susanta Adhikari,*[,†] Sandip Mandal,[‡,∥] Avijit Ghosh,[†,∥] Pradip Das,[§] and Debasis Das[‡]

[†]Department of Chemistry, University of Calcutta, 92, A.P.C. Road, Kolkata 700 009, West Bengal, India

[‡]Department of Chemistry, The University of Burdwan, Burdwan 713104, West Bengal, India

[§]Centre for Advanced Materials, Indian Association for the Cultivation of Science, Kolkata 700032, West Bengal, India

Supporting Information

ABSTRACT: A systematic journey from O-donor through S-donor to N-donor chelator led to the development of a highly selective Au^{3+} chemosensor that operates via a CHEF-induced FRET mechanism. This sensing protocol avoids unwanted possible side reactions observed in alkyne-based gold sensors. DFT studies strongly support the experimental facts. The probe **RT-2** detects Au^{3+} in the presence of the masking agent KI to minimize Hg^{2+} interference; however, **RQ-2** selectively detects Au^{3+} without any interference and shows reversibility in the sensing in the presence of tetrabutylammonium cyanide. The probe efficiently images Au^{3+} in living HeLa cells under a fluorescence microscope.

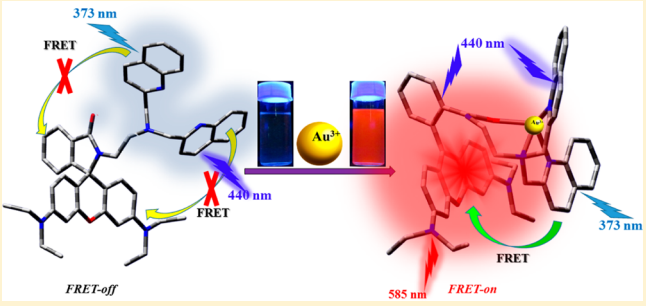

INTRODUCTION

Studies on the trace level determination of gold ion, an inhibitor of macrophages and polymorphonuclear leucocytes that suppress inflammation in rheumatic joints,[1] has gained immense importance for its unique optical,[2] catalytic,[3] and biocompatible[4] features. Moreover, it forms functional nanoparticles, useful for drug/gene delivery.[5] Gold-based drugs are used to combat a variety of diseases: viz., asthma, malaria, cancer, HIV, arthritis, and brain lesions.[6−9] Although metallic gold is highly biocompatible, its oxidized species (i.e., $Au^{+/\ 3+}$) are highly reactive and potentially toxic, causing serious damage to the liver, kidney, and peripheral nervous system.[10] In particular, Au^{3+} strongly binds to DNA/several enzymes leading to DNA cleavage and disruption of the nervous system.[11] Several gold ion selective "turn-on" fluorescence probes based on rhodamine,[12] BODIPY,[13] and naphthalimide[14] have been reported. Noticeably, most of them contain a reactive alkyne moiety appended to the fluorophore having a strong affinity to alkynophilic gold ion that leads to cyclization, hydration, or other irreversible chemical reactions[15,16] and are known as chemodosimeters.[17] On the other hand, rhodamine derivatives devoid of an alkyne unit, utilized for sensing cations and oxidative species, undergo transformation from the spirolactam (nonfluorescent) to open ring amide form (fluorescent) through a dosimetric approach and return to the original form in the presence of some metal chelating species, making the process reversible.[18] Thus, molecules of this class can be called chemosensors instead of conventional chemodosimeters. Obviously, the probes of this category are reusable and, hence, more desirable than chemodosimeters. Moreover, most of the reported probes face several shortcomings such as cross-sensitivity, slow response time, and weak fluorescence response that impede their optimum performance.[12a,15] Hence, the development of better gold sensors to overcome those limitations is highly demanding. The limited number of gold ion selective fluorescent chemosensors[12g,j,14b] leads to ample opportunity to develop more efficient and useful sensors for biological applications.

RESULTS AND DISCUSSION

The present probe senses Au^{3+} through a chelation enhanced fluorescence (CHEF) assisted fluorescence resonance energy transfer (FRET) process. FRET sensing is highly desirable in optical therapy, cell physiology, and analyte determination in biosystems. Moreover, spirocyclic rhodamine derivatives are extremely useful for selective analyte sensing due to their strong red emission, high quantum yield, cell permeability, and better performance as a FRET acceptor.[19] In intensity-based probes, the emission efficiency is highly dependent on the excitation intensity, probe concentration, and environment. FRET probes provide signals in the presence and absence of analyte to minimize those factors for accurate and quantitative detection of analyte.[20] Reports are available on Au^{3+}-selective ratiometric FRET probes having a reactive alkyl moiety appended to the fluorophore that function as chemodosimeters.[12k,14a] The present probe is weakly emissive due to the PET process. Upon binding with Au^{3+}, PET is inhibited due to the initiation of CHEF and consequently FRET starts. Thus, the present chemosensor functions via a CHEF-induced FRET mechanism.

Received: December 16, 2014
Published: August 7, 2015

DOI: 10.1021/acs.joc.5b01141
J. Org. Chem. 2015, 80, 8530−8538

Our initial strategy involving oxygen donors (e.g., furan-2-carboxaldehyde) appended to *N*-(rhodamine B) lactam-ethylenediamine for the detection of Au^{3+} was rather found to sense Al^{3+} selectively. Replacing oxygen with an S-donor (e.g., thiophene-2-carboxaldehyde) drastically changes the selectivity toward Au^{3+} along with Hg^{2+}, explicable in the light of a soft−soft interaction as per the HSAB principle.[21,22] This fact again encouraged us to switch over from an S-donor to an N-donor moiety, viz. quinoline, for its better FRET donor efficiency. Initial interference from Cr^{3+} has been eliminated using the bis-quinoline derivative instead of the mono-quinoline species for selective detection of Au^{3+}. The designed chemosensor suppresses the side reactions observed in the reaction-based probes where alkyne hydration and unusual hydroarylation occurs. Several probes based on quinoline (donor) and rhodamine (acceptor) conjugates, used for selective detection of Hg^{2+},[23] do not show the FRET process, probably due to the lack of favorable orientation of transition dipoles in those molecules.

The synthetic protocol of the present probes is shown in Schemes 1−4. The probe **RT-1** is synthesized by reductive

Scheme 1. Synthesis of Starting Compounds 1−3

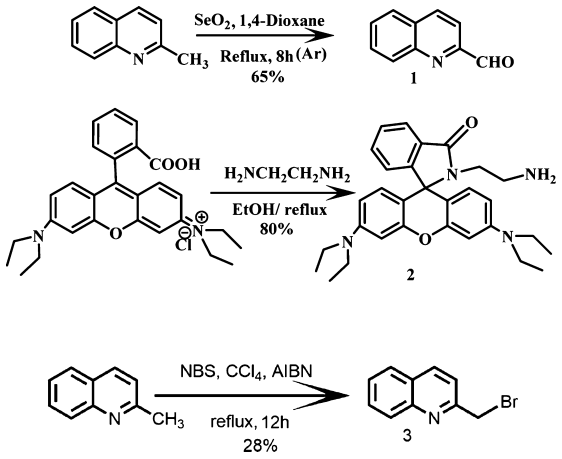

amination of *N*-(rhodamine B) lactam-ethylenediamine (**2**) with thiophene-2-carboxaldehyde, and further reductive amination of **RT-1** with thiophene-2-carboxaldehyde results in **RT-2**. The probes **RQ-1** and **RQ-2** are synthesized via reductive amination between rhodamine ethylenediamine and quinoline-2-carboxaldehyde (**1**) as mentioned above. Then, **RQ-2** is prepared in better yield by an alternate and improved method via N-alkylation of rhodamine ethylenediamine (**2**) with 2-(bromomethyl)quinoline (**3**). A model compound (**PAQ-2**) of the principal probe **RQ-2** has been prepared by N-alkylation of 2-picolylamine instead of rhodamine ethylenediamine using 2-(bromomethyl)quinoline (**3**). To further strengthen the sensing mechanism and establish the interaction feature of the appended quinoline moieties with Au^{3+} ion, another model compound (**RNap-2**) was synthesized. All of the probes and intermediates have been characterized by ^1H NMR, ^{13}C NMR, and QTOF-MS spectra (Figures S1−S19 in the Supporting Information).

While **RT-1** is Hg^{2+} selective (Figure S20 in the Supporting Information), **RT-2** senses Au^{3+}; however, Hg^{2+} interferes and hence is masked with KI.[19,21] On the other hand, **RQ-1** senses Au^{3+} with minor interference from Cr^{3+} (Figure S21 in the Supporting Information), while **RQ-2** is highly selective for

Scheme 2. Synthesis of Probes RT-1, RT-2, RQ-1, and RQ-2

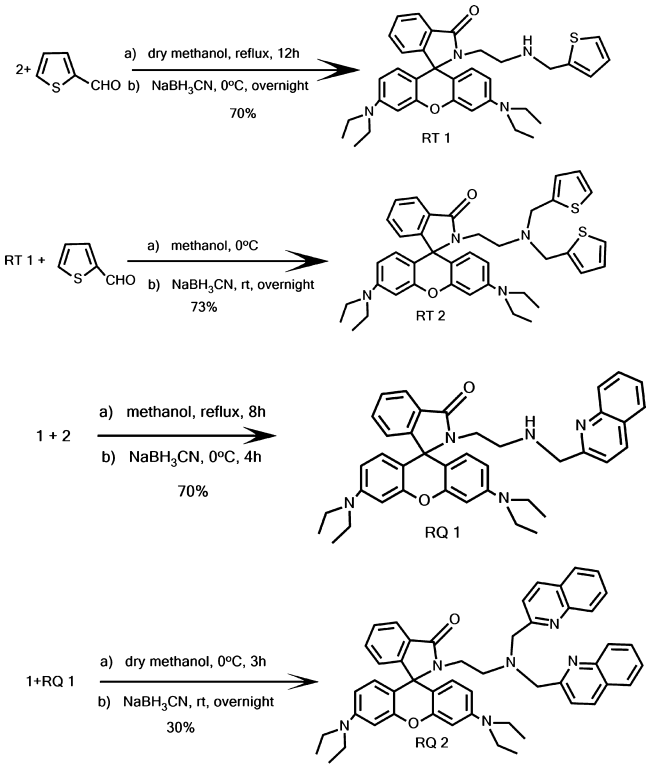

Scheme 3. Alternate Synthetic Pathway of RQ-2

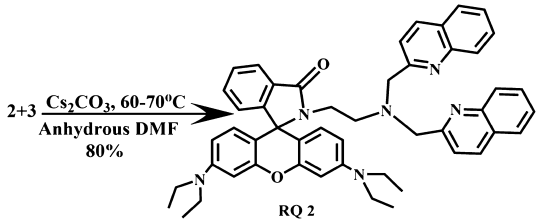

Scheme 4. Synthesis of the Model Compounds (a) PAQ-2 and (b) RNap-2

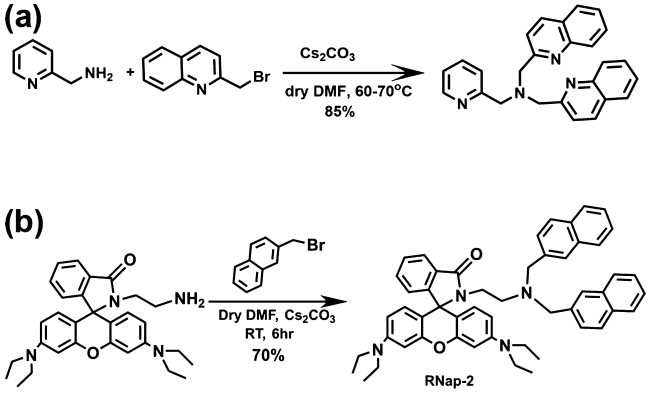

Au^{3+} with no interference. The emission of quinoline at ~450 nm being close to the absorbance of open ring rhodamine B moiety (~520 nm), with significant overlap and hence an efficient FRET process, is anticipated for both **RQ-1** and **RQ-2** in the presence of Au^{3+}. **RT-2** shows strong red fluorescence in the presence of both Hg^{2+} and Au^{3+} at 580 and 585 nm (slight

DOI: 10.1021/acs.joc.5b01141
J. Org. Chem. 2015, 80, 8530−8538

red shift), respectively (Figure 1). Interestingly, the sensing of Au^{3+} by **RQ-2** is reversible, as tetrabutylammonium cyanide

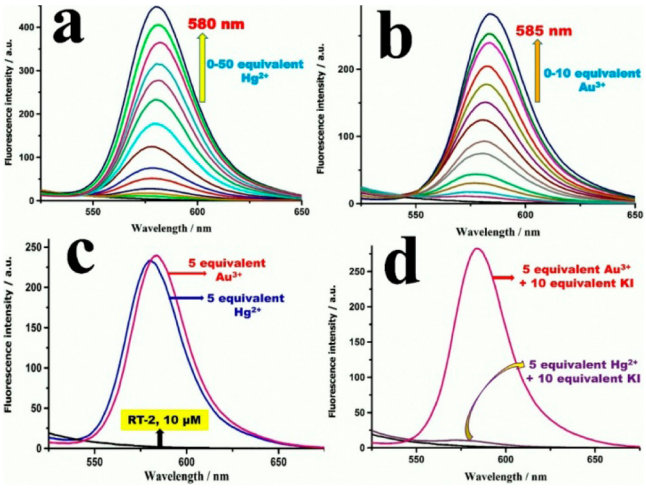

Figure 1. Changes in the emission spectra of **RT-2** (10 μM) upon gradual addition of (a) 0−50 equiv of Hg^{2+}, (b) 0−10 equiv of Au^{3+}, (c) 5 equiv of Hg^{2+} (blue line) and 5 equiv of Au^{3+} (red line), and (d) 5 equiv of Hg^{2+} + 10 equiv of KI (violet line) and 5 equiv of Au^{3+} + 10 equiv of KI (red line). Conditions: λ_{ex} 520 nm, ethanol/water 7/3 v/v, 0.1 M HEPES buffer, pH 7.4.

(TBACN) quenches the fluorescence of the adduct [**RQ-2**-Au^{3+}], leading to the generation of the free probe.

Naked-eye and UV-light-exposed colors of Hg^{2+} and Au^{3+} adducts of **RT-2** in the presence and absence of KI are presented in Figure S22 in the Supporting Information. Both **RQ-1** and **RQ-2** are weakly emissive (λ_{em} 440 nm, λ_{ex} 373 nm), probably due to the PET process from the N-donor of the spirolactam ring to the quinoline moiety.[19a] Addition of Au^{3+} enhances the emission intensity at 440 nm due to inhibition of PET with initiation of CHEF. As soon as CHEF occurs, the spirolactam ring opens, allowing quinoline and rhodamine units to come closer to initiate the FRET process. The spectral overlap between donor (quinoline) emission and acceptor absorbance (open ring rhodamine B) is shown in Figure 2.

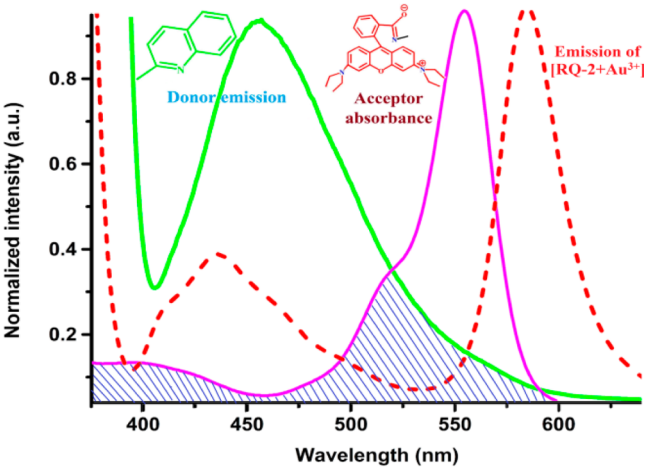

Figure 2. Spectral overlap between donor emission (quinoline; green) and acceptor absorbance (open ring rhodamine B; pink). The dotted line (red) shows the emission spectrum of the adduct [**RQ-2**+Au^{3+}].

Figure 3a reveals the high selectivity of **RQ-2** for Au^{3+}, and the corresponding naked-eye and UV-light-exposed colors are presented in Figure S23 in the Supporting Information. Figure 3b,c indicates that the emission intensities of **RQ-2** at 440 nm (due to the quinoline moiety) and 585 nm (due to the open ring rhodamine unit) increases with increasing Au^{3+} concentration. This means that, as soon as Au^{3+} initiates the CHEF process, the PET stops and, simultaneously, the FRET process starts. To further support this fact, th emodel compound **PAQ-2** was prepared (Scheme 4a), replacing the rhodamine unit of **RQ-2** with a picolyl moiety. At first the emission properties of **PAQ-2** were investigated in the presence and absence of Au^{3+} at pH 7.4 (Figure S24 in the Supporting Information). The enhancement of emission intensity of **PAQ-2** in the presence of Au^{3+} allows the conclusion that Au^{3+} initiates the CHEF process through inhibition of PET. In addition to this fact, the compound **RNap-2** (Scheme 4b) having a rhodamine unit with no appended chelator (i.e., quinolone) exhibits insignificant change in emission in the presence of Au^{3+} (Figure S25 in the Supporting Information), thereby indicating the key role of appended quinolines (in **RQ-2**) in the selective sensing of Au^{3+}.

At lower pH (pH 2.0−4.0) the spirolactam ring of the rhodamine unit opens, which results in strong red emission as usual. The effect of pH (pH 2.0−6.0) on the emission properties of **RQ-2** and **PAQ-2** in the presence of Au^{3+} has been thoroughly investigated (Figure S26 in the Supporting Information). For both molecules, the emission intensity of the quinoline unit does not increase significantly upon addition of Au^{3+} at pH 2.0, probably due to protonation of its "N" center. The emission intensity of the quinoline unit increases slightly at pH 3.0 and above. Thus, the quinoline "N" center is more susceptible to protonation at low pH than spirolactam ring opening. Therefore, on the basis of this fact, the sensing mechanism is attributed to a CHEF-assisted FRET process, particularly at physiological pH. Figure S27 in the Supporting Information displays the reversibility of Au^{3+} complexation upon gradual addition of CN^- in the form of TBACN to the solution of the adduct [**RQ-2**+Au^{3+}]. The corresponding naked-eye color change from the red complex [**RQ-2**-Au^{3+}] to colorless is shown in Figure S28 in the Supporting Information. The quenching of the fluorescence and absorbance of the ensemble indicated the closing of the lactam ring in **RQ-2**.

The detection limit for Au^{3+} is 0.5 nM, much lower than that of existing probes (Table S1 in the Supporting Information).[12−15] Naked-eye and UV-light-exposed colors of **RQ-2** in the presence of Au^{3+} are shown in Figure S29 in the Supporting Information. A bar diagram showing the emission intensities of **RQ-2** and **RQ-2**-Au^{3+} adduct in the presence of common cations are shown in Figure S30 in the Supporting Information. Figure 3b (inset) shows the plot of emission intensity vs Au^{3+} concentration, the linear region (up to 10 μM Au^{3+}) of which (Figure 3d and up to 0.5 nM in Figure S31 in the Supporting Information) is useful for the determination of unknown Au^{3+} concentration. Changes in absorbance of **RQ-2** upon gradual addition of Au^{3+} (at 556 nm) are presented in Figure S32 in the Supporting Information, attributed to the Au^{3+} assisted spirolactam ring opening. The effect of pH on the emission intensities of free **RQ-2** and **RQ-2**-Au^{3+} systems (Figure S33 in the Supporting Information) indicates the optimum pH for Au^{3+} detection ranges from 4.0 to 10.0. The free energy for hydration for Au^{3+} is ∼−4420 kJ/mol, which suggests that Au^{3+} will be favorably solvated with increasing water content

DOI: 10.1021/acs.joc.5b01141
J. Org. Chem. 2015, 80, 8530−8538

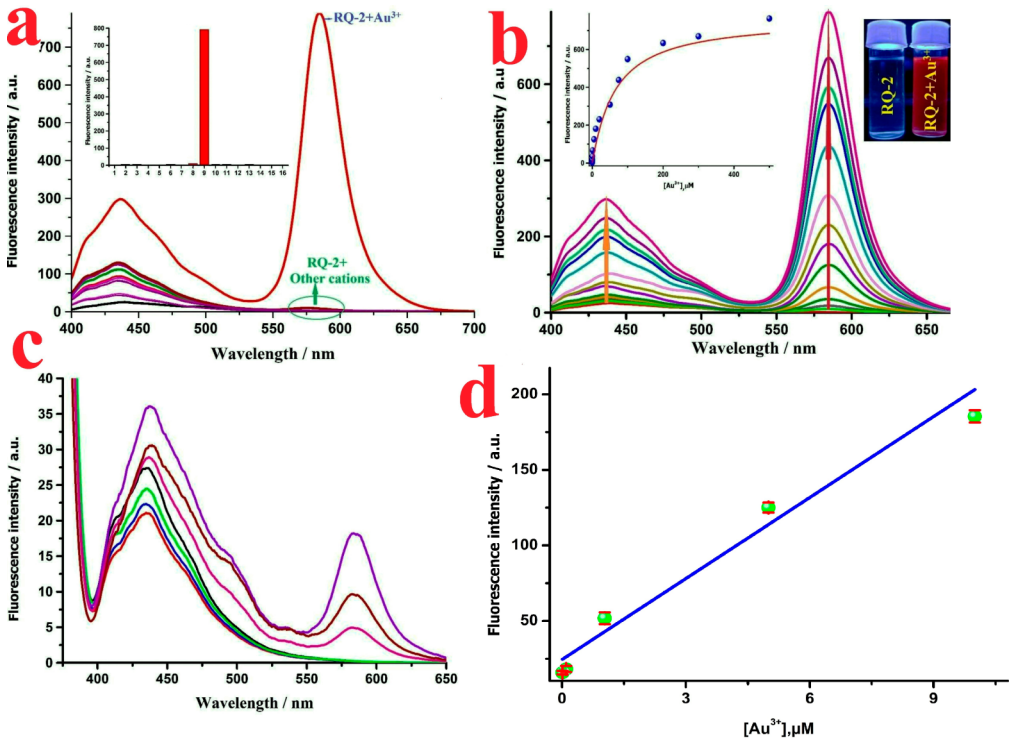

Figure 3. Changes in the emission spectra of **RQ-2** (10 μM): (a) upon addition of 50 equiv of Au^{3+} and other cations (inset: emission intensities of free **RQ-2** (1) and its adduct with Hg^{2+} (2), Zn^{2+} (3), Pb^{2+} (4), Ca^{2+} (5), Ag^{+} (6), Co^{2+} (7), Au^{+} (8), Au^{3+} (9), Fe^{3+} (10), Mg^{2+} (11), Mn^{2+} (12), Cu^{2+} (13), Cd^{2+} (14), Cr^{3+} (15) and Al^{3+} (16)); (b) upon gradual addition of Au^{3+} (0.0, 0.05, 0.1, 0.5, 1.0, 5.0, 10.0, 20.0, 50.0, 75.0, 100.0, 200.0, 300.0, and 500.0 μM) (inset: emission intensity vs Au^{3+} concentration); (c) at low Au^{3+} concentration (0.0, 0.0005, 0.001, 0.005, 0.01, 0.05, and 0.1 μM); (d) linear region of the inset of Figure 3b (up to 10 μM Au^{3+}). Conditions: 7/3 (v/v) ethanol/water, 0.1 M HEPES buffer, pH 7.4, λ_{ex} 373 nm. Error bar: n = 3.

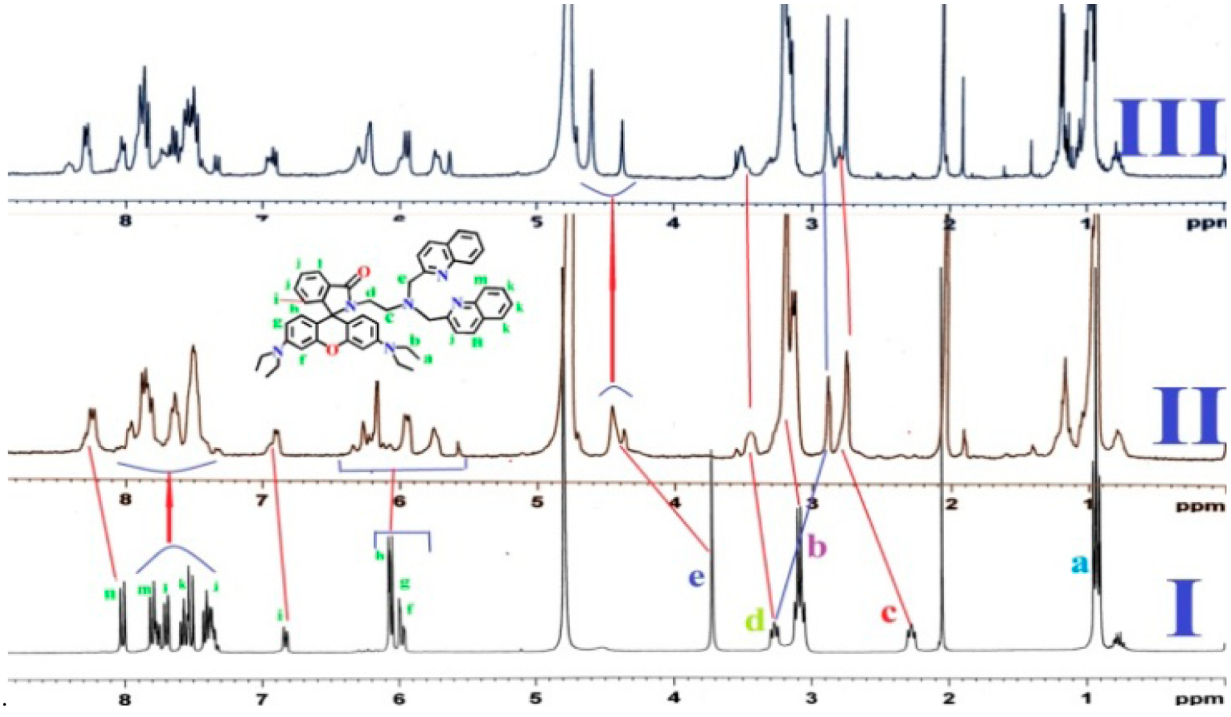

Figure 4. ^{1}H NMR spectral changes of **RQ-2**: (I) free **RQ-2**; (II) **RQ-2** + 1.0 equiv of Au^{3+}; (III) **RQ-2** + 1.0 equiv of Au^{3+} in methanol-d_4 after 20 min.

(Figures S34 and S35 in the Supporting Information), and it is observed that ethanol/water 7/3 (v/v) in 0.1 M HEPES buffer at pH 7.4 are the optimum conditions for Au^{3+}detection. A Job plot (Figure S36 in the Supporting Information) indicates 1:1 stoichiometry of the [**RQ-2**-Au^{3+}] adduct. The binding constant of **RQ-2** for Au^{3+} is calculated using the Benesi–

DOI: 10.1021/acs.joc.5b01141
J. Org. Chem. 2015, 80, 8530−8538

Hildebrand equation,[24] $(F_{max} - F_0)/(F_x - F_0) = 1 + (1/K)(1/[M]^n)$, where F_{max}, F_0, and F_x are fluorescence intensities of **RQ-2** in the presence of Au^{3+} at saturation, free **RQ-2**, and any intermediate Au^{3+} concentration (Figure S37 in the Supporting Information). A plot of $(F_{max} - F_0)/(F_x - F_0)$ vs $1/[M]^1$ (here $n = 1$) yields an apparent binding constant of 8.9×10^4 M^{-1} ($R^2 = 0.995$).

In order to strengthen the above mechanism, ^1H NMR titration has been performed by adding Au^{3+} to the methanol-d_4 solution of **RQ-2** (Figure 4). A significant spectral change in **RQ-2** has been observed upon addition of Au^{3+}. After addition of 1 equiv of of Au^{3+} (Figure 4II), two "e" protons of quinoline have shifted downfield about 0.66 ppm (3.72 to 4.38 ppm), while the "**c**" proton is also shifted downfield from 2.26 to 2.76 ppm. The "d" protons of the ethylenediamine linker have been shifted to two positions at 2.89 (upfield) and 3.46 ppm (downfield). This shift is attributed to Au^{3+}-assisted spirolactam ring opening of **RQ-2** followed by rotation of the molecule. The aromatic protons of quinoline moieties "m" and "n" have also shifted significantly downfield by 0.08 ppm (7.74 to 7.82 ppm) and 0.24 ppm (7.99 to 8.23 ppm), respectively, clearly indicating the coordination of quinoline "N" donors to Au^{3+}. The protons of rhodamine unit "h" and "I" have also shifted downfield to 6.27 and 6.91 ppm from 6.06 and 6.84 ppm, respectively. After 20 min (Figure 4III), "h" and "I" protons further shifted to 6.30 and 6.94 ppm, respectively, indicating molecular rotation and initiation of the FRET process. The other remaining protons have also been shifted to some extent. Significant proton shifts are noted in Table S2 (Supporting Information). Formation of the **RQ-2**-Au^{3+} adduct is also demonstrated from its mass spectrum, which shows m/z 481.05, attributed to the fragment $[\mathbf{RQ\text{-}2}+Au^{3+}\text{-}H^+]^{2+}/2$ (Figure S38 in the Supporting Information).

DFT studies further support the Au^{3+}-assisted FRET ON process in **RQ-2**. The optimized geometries of **RQ-2** (Figure S39 in the Supporting Information) and **RQ-2**-Au^{3+} adduct (Figure S40 in the Supporting Information) have been generated using 6-31G/LanL2DZ and B3LYP/LanL2DZ basis sets, respectively, with Gaussian 09 software.[25] Table S3 in the Supporting Information presents frontier molecular orbitals of **RQ-2** along with their energy levels. **RQ-2** has an extended form due to the two-carbon spacer, while the **RQ-2**-Au^{3+} adduct is relatively compact. The coordination of Au^{3+} with oxygen and nitrogen donors of **RQ-2** brings quinoline groups close to the rhodamine unit. Selected bond distances and bond angles of the **RQ-2-Au**$^{3+}$ adduct are presented in Table S4 in the Supporting Information. The interaction of **RQ-2** with Au^{3+} affects the HOMO/LUMO energy levels of quinoline and rhodamine chromophores. When the lactam ring is closed, the HOMO−LUMO energy gap of the acceptor (rhodamine unit) is greater than that of the quinoline donor, suppressing the energy transfer from quinoline to rhodamine. As **RQ-2** binds Au^{3+} and the spirolactam ring opens, the energy gap in the rhodamine unit markedly reduces to match that of the quinoline unit, enabling an intramolecular FRET process. The efficiency of energy transfer from the quinoline to the rhodamine unit has also been calculated using the equation[26] $E = 1 - (F_{DA}/F_D)$, where F_{DA} and F_D represent emission intensities of the donor in the presence and absence of acceptor, respectively. The calculated value in the presence of Au^{3+} (5 μM) is 0.52 (Figure S41 in the Supporting Information)

The excited state related calculations of the **RQ-2-Au**$^{3+}$ adduct have been carried out using time-dependent DFT (TDDFT), on the basis of the optimized ground state geometry. From the calculated data, both the LUMO and LUMO+1 of **RQ-2**-Au^{3+} adduct are localized on the quinoline units, while the HOMO and HOMO-1 are localized on the donor rhodamine unit (Table S5 in the Supporting Information). From an energy point of view, two main allowed electronic transitions have been observed for **RQ-2-Au**$^{3+}$: viz. HOMO → LUMO (2.1193 eV, 585.03 nm, $f = 0.6570$) and HOMO-1 → LUMO+1 (549 nm, 2.2193 eV, $f = 0.6875$) (Table S6 in the Supporting Information). The calculated coefficient of the wave function (CI) for the HOMO-1 to LUMO+1 transition is 0.8342, which indicates that radiative decay is possible and eventually leads to emission from **RQ-2-Au**$^{3+}$ adduct. Moreover, the calculated energy difference between HOMO-1 and LUMO+1 (2.28 eV) of **RQ-2** -Au^{3+} is lower than that of the free **RQ-2** (the HOMO to LUMO energy gap is 3.21 eV) (Figure 5). Hence, the complexation between **RQ-2** and Au^{3+} is also energetically favorable.

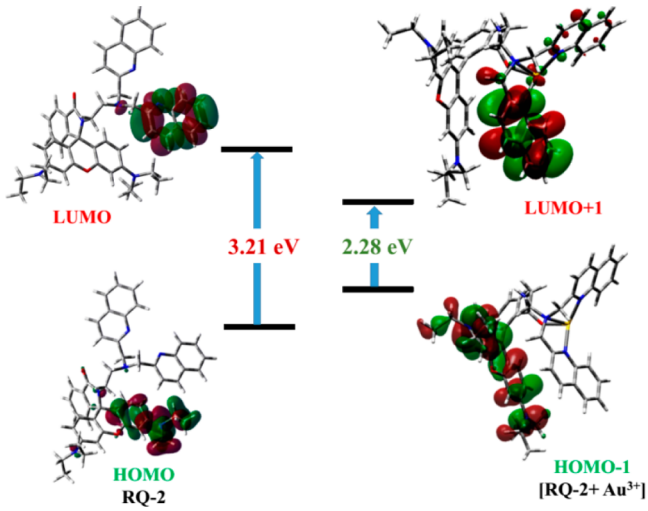

Figure 5. HOMO−LUMO and HOMO-1−LUMO+1 energy gaps in **RQ-2** and **RQ-2-Au**$^{3+}$ adduct.

Thus, the above discussion supported by spectroscopic evidence and theoretical TDDFT studies allowed us to portray the plausible Au^{3+} sensing mechanism by **RQ-2**, as shown in Figure 6.

Intracellular Au^{3+} imaging using **RQ-2** on HeLa cells has been investigated. The cells were incubated with 20 μM Au^{3+} for 1h. Then the cells were washed three times with PBS buffer and **RQ-2** was added to the medium followed by further incubation for 30 min. Figure 7 reveals that **RQ-2** is cell-permeable to efficiently image intracellular Au^{3+} under a fluorescence microscope.

The cytotoxicity of **RQ-2** on HeLa cells was determined by an MTT assay (Supporting Information). Upon exposure of 10 μM **RQ-2** for 12 h, ~90% of the HeLa cells remained viable (Figure 8). This nullifies the possibility of any significant cytotoxic influence of **RQ-2** on HeLa cells. Therefore, **RQ-2** may be used as an ideal chemosensor for Au^{3+} in living systems.

CONCLUSION

In summary, we have designed and synthesized a series of rhodamine-based compounds, out of which **RQ-2** has been

DOI: 10.1021/acs.joc.5b01141
J. Org. Chem. 2015, 80, 8530−8538

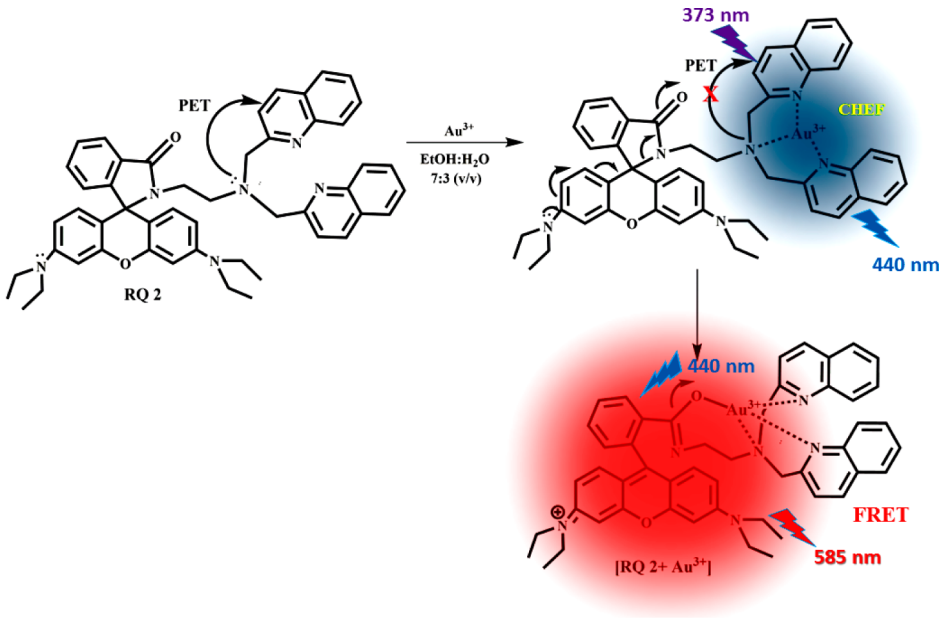

Figure 6. Probable Au^{3+} sensing mechanism of **RQ-2** via CHEF-induced FRET process.

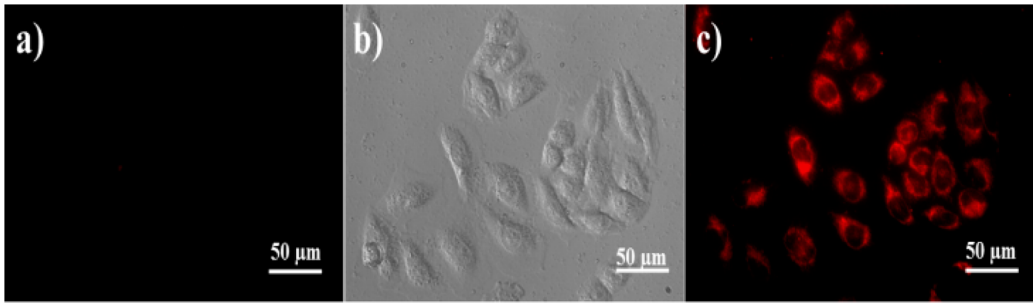

Figure 7. Imaging of Au^{3+} in HeLa cells: (a) fluorescence image of the cells after incubation only with **RQ-2** (10 μM); (b) bright field image of those cells; (c) fluorescence image of the cells after incubation with 20 μM Au^{3+} followed by addition of 10 μM **RQ-2**. Fluorescence imaging of cells was performed under green light (480−550 nm) excitation, with fluorescence signals collected in the range >590 nm. **RQ-2** was prepared in ~0.3% ethanol in water.

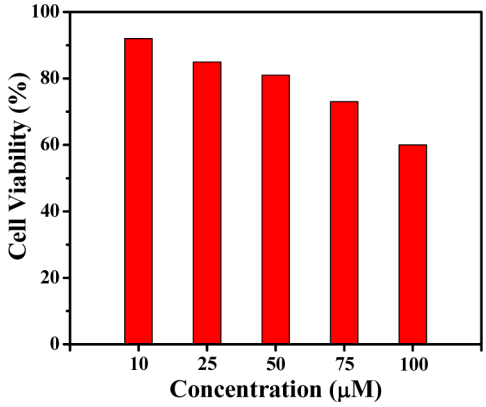

Figure 8. Cell viability of **RQ-2** at different concentrations against HeLa cells after 12 h incubation.

established as an excellent probe for detection of trace level Au^{3+}. A systematic approach to tune the receptor sites has been pursued for highest selectivity toward Au^{3+}. Systematic variation of donor sites from O through S to N allowed us to achieve higher Au^{3+} selectivity that operates via a CHEF-assisted FRET mechanism. Thus, **RQ-2** shows higher sensitivity as well as faster response time in comparison to those reported systems where the interaction of the alkyne unit with gold ion is the major focus. Thus, the present demonstration is a new addendum for gold ion sensing in the horizon of rhodamine-based receptors. Furthermore, the probe is cell-permeable and is able to detect Au^{3+} ion in living cells.

EXPERIMENTAL SECTION

Materials and Equipment. All metal salts were used as either their nitrate or their chloride salts except for tetrabutylammonium cyanide. Other chemicals were of analytical reagent grade and were used without further purification except when specified. ^{1}H NMR spectra were recorded at 300 and 75 MHz for ^{13}C NMR using the solvent peak as an internal reference at 25 °C. Thin-layer chromatography (TLC) was carried out on 0.25 mm thick precoated silica plates, and spots were visualized under UV light. IR spectra were determined on a spectrophotometer. Absorption and fluorescence spectra were recorded on an UV−vis spectrometer and on a spectrofluorimeter at room temperature. HRMS analysis was performed in a QTOF mass analyzer using the ionization method detailed in the Supporting Information.

Synthesis. *Quinoline-2-carbaldehyde (1).* Quinoline-2-carbaldehyde was prepared according to literature methods.[27] Selective oxidation of 2-methylquinolone (2.0 g, 13.968 mmol) with 4 equiv of selenium dioxide (SeO_2) in dioxane for 24 h afforded 1.427 g of

DOI: 10.1021/acs.joc.5b01141
J. Org. Chem. 2015, 80, 8530−8538

quinoline-2-carboxaldehyde in 65% yield. The oxidation reaction was smooth, except for the tedious removal of the dioxane solvent from the compound.

*2-(2-Aminoethyl)-3′,6′-bis(diethylamino)spiro[isoindoline-1,9′-xanthen]-3-one (**2**).* A portion of rhodamine B (5.0 g, 10.438 mmol) was mixed with 2 equiv of ethylenediamine in ethanol and refluxed for 12 h to give 4.047 g (yield 80%) of *N*-(rhodamine B) lactam-ethylenediamine as a reddish brown solid.[28] The solid was crystallized from acetonitrile.

*2-(Bromomethyl)quinoline (**3**).* 2-(Bromomethyl)quinoline was prepared by the published method.[29] The solid obtained was purified by column chromatography in a yield of 28% and characterized by ^{1}H NMR (Figure S1 in the Supporting Information). ^{1}H NMR (300 MHz, $CDCl_3$): δ 4.706 (2H, s), 7.510−7.563 (2H, m), 7.688−7.745 (1H, m), 7.791 (1H, m), 8.065 (1H, d, J = 8.4 Hz), 8.146 (1H, d, J = 8.4 Hz).

*3′,6′-Bis(diethylamino)-2-(2-((thiophen-2-ylmethyl)amino)ethyl)-spiro[isoindoline-1,9′-xanthen]-3-one (**RT-1**).* A 300 mg portion of **2** (0.619 mmol) and 69.42 mg of thiophene-2-carboxaldehyde (0.619 mmol) were taken up in dry methanol and refluxed for 12 h under an argon atmosphere. After completion of the reaction monitored by TLC, the reaction mixture was cooled to room temperature. Then 116.73 mg of sodium cyanoborohydride (1.857 mmol) was added by portion at 0 °C. Then the reaction mixture was stirred for 5 h at room temperature. After completion of the reaction was confirmed by TLC, the solvent was removed under vacuum and water was added carefully to the reaction mixture. The reaction mixture was extracted with ethyl acetate (twice), washed with brine, and dried over anhydrous sodium sulfate. Then the solvent was rotary evaporated to give a yellow oil. The crude product was purified by column chromatography using 20% ethyl acetate−80% petroleum ether as eluent to afford a light yellow liquid (255 mg, yield: 70%). R_f = 0.25 in 30% ethyl acetate−70% petroleum ether. ^{1}H NMR (Figure S2 in the Supporting Information) (300 MHz, $CDCl_3$): δ 7.88−7.90 (m, 1H), 7.41−7.45 (m, 2H), 7.05−7.12 (m, 2H), 6.84−6.87 (m, 1H), 6.77−6.78 (m, 1H), 6.36−6.43 (m, 4H), 6.22−6.26 (m, 2H), 3.73 (s, 2H), 3.28−3.36 (m, 10H), 2.44 (t, 6.3 Hz, 2H),1.15 (m, 12H); ^{13}C NMR (Figure S3 in the Supporting Information) (75 MHz, $CDCl_3$): δ 168.5, 153.6, 153.3, 148.8, 144.0, 132.3, 131.1, 128.7, 127.9, 126.4, 124.6, 124.0, 123.7, 122.7, 108.1, 105.6, 97.8, 64.9, 47.7, 47.2, 44.3, 39.9, 12.6. QTOF MASS (Figure S4 in the Supporting Information): m/z (M + H)$^+$ calculated for $C_{35}H_{41}N_4O_2S^+$ 581.2950, found 581.2950.

*2-(2-(Bis(thiophen-2-ylmethyl)amino)ethyl)-3′,6′-bis-(diethylamino)spiro[isoindoline-1,9′-xanthen]-3-one (**RT-2**).* A 400 mg portion of **RT-1** (0.688 mmol) and 77.15 mg of thiophene-2-carboxaldehyde (0.688 mmol) were taken up in dry methanol and stirred at 0 °C under an argon atmosphere for 3 h. Then 129.74 mg of sodium cyanoborohydride (2.064 mmol) was added by portion at 0 °C. Then the reaction mixture was stirred for 5 h at room temperature. After completion of the reaction was confirmed by TLC, the solvent was removed under vacuum and water was added carefully to the reaction mixture. The reaction mixture was extracted with ethyl acetate (twice) and dried over anhydrous sodium sulfate. Then the solvent was rotary evaporated to give a brown oil. The crude product was purified by column chromatography using 40% ethyl acetate−60% petroleum ether as eluent to give a light yellow liquid (340 mg, yield: 73%). R_f = 0.35 in 40% ethyl acetate−60% petroleum ether. ^{1}H NMR (Figure S5 in the Supporting Information) (300 MHz, $CDCl_3$): δ 7.89−7.91 (m, 1H), 7.41−7.44 (m, 1H), 7.15−7.27 (m, 2H), 7.06−7.09 (m, 1H), 6.89−6.97 (m, 4H), 6.79−6.80 (m, 1H), 6.40−6.44 (m, 4H), 6.25−6.37 (m, 2H), 4.77 (s, 4H), 3.32−3.36 (m, 10H), 2.34 (m, 2H), 1.18 (m, 12H). ^{13}C NMR (Figure S6 in the Supporting Information) (75 MHz, $CDCl_3$): δ 168.1, 167.9, 153.6, 153.3, 148.9, 148.8, 144.4, 141.8, 141.0, 137.9, 132.5, 132.3, 128.9, 128.8, 128.1, 126.8, 126.6, 126.5, 125.9, 125.6, 125.2, 124.6, 123.8, 122.8, 115.3, 108.3, 105.5, 97.9, 97.8, 65.1, 59.7, 53.9, 51.1, 51.0, 50.7, 49.2, 44.4, 38.6, 38.2, 12.7. QTOF MASS (Figure S7 in the Supporting Information): m/z (M + H)$^+$ calculated for $C_{40}H_{45}N_4O_2S_2^+$ 677.2983, found 677.2987.

*3′,6′-Bis(diethylamino)-2-(2-((quinolin-2-ylmethyl)amino)ethyl)-spiro[isoindoline-1,9′-xanthen]-3-one (**RQ-1**).* A 300 mg portion of **2** (0.619 mmol) and 97.28 mg of **1** (0.619 mmol) were taken up in dry methanol and refluxed for 12 h under an argon atmosphere. After completion of the reaction was monitored by TLC, the reaction mixture was cooled to room temperature. Then 116.73 mg of sodium cyanobhorohydride (1.857 mmol) was added by portion at 0 °C. Then the reaction mixture was stirred for 5 h at room temperature. After completion of the reaction was confirmed by TLC, the solvent was removed under vacuum and water was added carefully to the reaction mixture. The reaction mixture was extracted with ethyl acetate (twice) and dried over anhydrous sodium sulfate. Then the organic layer was vacuum-evaporated to give a brown oil. The crude product was purified by column chromatography using 40% ethyl acetate−60% petroleum ether as eluent to give a deep yellow solid (274 mg, yield: 70%). R_f = 0.35 in 60% ethyl acetate−40% petroleum ether. Mp: 62 °C. ^{1}H NMR (Figure S8 in the Supporting Information) (300 MHz, $CDCl_3$): δ 7.97−8.06 (m, 2H), 7.91−7.92(m, 1H), 7.74−7.77 (m, 1H), 7.62−7.67 (m, 1H), 7.36−7.49 (m, 4H), 7.05−7.08 (m, 1H), 6.40−6.43 (m, 2H), 6.34 (s, 2H), 6.15−6.19 (m, 2H), 3.90 (s, 2H), 3.24−3.36 (m, 8H), 2.54(m, 2H), 1.13 (m, 12H); ^{13}C NMR (Figure S9 in the Supporting Information) (75 MHz, $CDCl_3$): δ 171.0, 153.6, 153.2, 148.7, 147.5, 136.1, 132.2, 129.1, 128.9, 128.7, 127.9, 127.3, 125.8, 123.7, 122.7, 120.3, 108.0, 105.5, 97.8, 65., 55.0, 47.8, 44.2, 12.5. QTOF MASS (Figure S10 in the Supporting Information): m/z (M + H)$^+$ calculated for $C_{40}H_{44}N_5O_2^+$ 626.3495, found 626.3487.

*2-(2-(Bis(quinolin-2-ylmethyl)amino)ethyl)-3′,6′-bis-(diethylamino)spiro[isoindoline-1,9′-xanthen]-3-one (**RQ-2**). Method A.* A 300 mg portion of **RQ-1** (0.479 mmol) and 75.34 mg of **1** (0.479 mmol) were taken up in dry methanol and stirred at 0 °C under an argon atmosphere for 3 h. Then 90.40 mg of sodium cyanobhorohydride (1.437 mmol) was added by portion at 0 °C. Then the reaction mixture was stirred for 5 h at room temperature. After completion of the reaction was confirmed by TLC, the solvent was removed under vacuum and water was added carefully to the reaction mixture. The reaction mixture was extracted with ethyl acetate (twice) and dried over anhydrous sodium sulfate. Then the solvent was vacuum-evaporated to give a brown oil. The crude product was purified by column chromatography using 40% ethyl acetate−60% petroleum ether as eluent to give a light yellow solid (111 mg, yield: 30%). R_f = 0.35 in 40% ethyl acetate−60% petroleum ether. Mp: 80 °C. ^{1}H NMR (Figure S11 in the Supporting Information) (300 MHz, $CDCl_3$): δ 7.89−8.02 (m, 5H), 7.57−7.71 (m, 6H), 7.37−7.44 (m, 4H), 7.01−7.04 (m, 1H), 6.31−6.34 (m, 2H), 6.23 (s, 2H), 6.07−6.11 (m, 2H), 3.90 (s, 4H), 3.46−3.51 (m, 2H), 3.17−3.23 (m, 8H), 2.47 (m, 2H), 1.09 (m, 12H). ^{13}C NMR (Figure S12 in the Supporting Information) (75 MHz, $CDCl_3$): δ 170.9, 162.3, 160.4, 153.3, 153.2, 148.6, 147.4, 136.0, 132.1, 131.3, 128.9, 128.9, 127.8, 127.3, 127.2, 125.7, 123.7, 122.5, 120.8, 107.9, 105.5, 97.6, 64.8, 60.7, 60.2, 52.8, 44.1, 12.5. QTOF MASS (Figure S13 in the Supporting Information): m/z (M + H)$^+$ calculated for $C_{50}H_{51}N_6O_2^+$ 767.4073, found 767.4073.

Method B. A 300 mg portion of **2** (0.619 mmol) and 274.93 mg of **3** (1.238 mmol) were taken up in 2 mL of dry DMF, and 806 mg of Cs_2CO_3 (2.476 mmol) was added to the mixture under an argon atmosphere in the dark. Then the reaction mixture was stirred at room temperature overnight in the dark. After completion of the reaction was confirmed by TLC, the reaction mixture was quenched with cold bicarbonate solution. The reaction mixture was extracted with 30 mL of ethyl acetate (three times) and washed with cold brine solution. The organic part was dried over anhydrous sodium sulfate and vacuum-evaporated to give a brown oil. The crude product was purified by column chromatography using 30% ethyl acetate−70% petroleum ether as eluent to give a light yellow solid (384 mg, yield 80%). R_f = 0.35 in 40% ethyl acetate−60% petroleum ether.

*1-(Pyridin-2-yl)-N,N-bis(quinolin-2-ylmethyl) methanamine (**PAQ-2**).* A 100 mg portion of pyridin-2-ylmethanamine (0.926 mmol) and 409 mg of **3** (1.852 mmol) were taken up in 2 mL of dry DMF, and 1.206 g of Cs_2CO_3 (3.704 mmol) was added to the mixture under an argon atmosphere in dark. Then the reaction mixture was stirred at room temperature overnight in the dark. After completion of

DOI: 10.1021/acs.joc.5b01141
J. Org. Chem. 2015, 80, 8530−8538

the reaction was confirmed by TLC, the reaction mixture was quenched by cold bicarbonate solution. Then the mixture was extracted with 30 mL of ethyl acetate (three times) and washed with cold brine solution. The organic part was dried over anhydrous sodium sulfate and vacuum-evaporated to give a brown oil. The crude product was purified by column chromatography using 30% ethyl acetate−70% petroleum ether to obtain a light yellow solid (307 mg, yield: 85%). R_f = 0.35 in 40% ethyl acetate−60% petroleum ether. Mp: 82 °C. The target product was confirmed by ^{1}H NMR (Figure S14 in the Supporting Information) (300 MHz, $CDCl_3$): δ 3.986 (s, 2H), 4.106 (s, 4H), 7.111 (d, 1H), 7.457 (d, 2H), 7.646 (m, 4H), 7.757 (m, 4H), 8.088 (m, 4H), 8.540 (d, 1H). ^{13}C NMR (Figure S15 in the Supporting Information) (75 MHz, $CDCl_3$): δ 60.25, 60.82, 120.84, 121.80, 122.98, 125.90, 127.16, 129.03, 136.09, 147.38, 148.87, 159.04, 159.86, 162.20. QTOF MASS (Figure S16 in the Supporting Information): m/z $(M + H)^+$ calculated for $C_{26}H_{23}N_4^+$ 391.1922, found 391.1922.

2-(2-(Bis(naphthalen-2-ylmethyl)amino)ethyl)-3′,6′-bis(diethylamino)spiro[isoindoline-1,9′-xanthen]-3-one (**RNap-2**). A 221 mg portion of 2-(bromomethyl)naphthalene (0.999 mmol) and 241 mg of **3** (0.499 mmol) were taken up in 2 mL of dry DMF, and 977 mg of Cs_2CO_3 (2.99 mmol) was added to the mixture under an argon atmosphere. Then the reaction mixture was stirred at room temperature for 6 h. After completion of the reaction was confirmed by TLC, the reaction mixture was quenched by cold brine solution. Then the mixture was extracted using 30 mL ethyl acetate (three times) and washed with cold brine solution. The organic part was dried over anhydrous sodium sulfate and vacuum-evaporated to give a deep yellow oil. The crude product was purified by column chromatography using 30% ethyl acetate−70% petroleum ether to obtain a light yellow liquid (300 mg, yield: 78%). R_f = 0.30 in 30% ethyl acetate−70% petroleum ether. ^{1}H NMR (Figure S17 in the Supporting Information) (300 MHz, $CDCl_3$): δ 7.97 (m, 1H), 7.57−7.71 (m, 6H), 7.80−7.83 (m, 3H), 7.75 (m, 2H), 7.69 (m, 2H), 7.43−7.45 (m, 8H), 7.07 (m, 1H), 6.40−6.43 (m, 2H), 6.40−6.43 (m, 2H), 6.25 (m, 2H), 3.711 (m, 4H), 3.50 (m, 2H), 3.21−3.27 (m, 8H), 2.47 (m, 2H), 1.12 (m, 12H); ^{13}C NMR (Figure S18 in the Supporting Information) (75 MHz, $CDCl_3$): δ 167.6, 153.5, 153.3, 148.6, 137.0, 133.4, 132.7, 132.2, 131.6, 128.8, 128.0, 127.8, 127.7, 127.6, 127.2, 127.1, 125.7, 125.3, 123.8, 122.6, 122.6, 108.0, 105.7, 97.8, 64.9, 57.6, 51.9, 46.3, 44.2, 37.98, 12.5. QTOF MASS (Figure S19 in the Supporting Information) m/z $(M + H)^+$ calculated for $C_{52}H_{53}N_4O_2^+$ 765.4168, found 765.4164.

■ ASSOCIATED CONTENT

Supporting Information

The Supporting Information is available free of charge on the ACS Publications website at DOI: 10.1021/acs.joc.5b01141.

^{1}H and ^{13}C NMR and HRMS spectra of all probes, DFT calculations, experimental details and room-temperature absorption and fluorescence spectra for the probes, and Cartesian coordinates and absolute energy values for the optimized geometries (PDF)

■ AUTHOR INFORMATION

Corresponding Author

*E-mail for S.A.: adhikarisusanta@yahoo.com.

Author Contributions

‖These authors contributed equally to this work.

Notes

The authors declare no competing financial interest.

■ ACKNOWLEDGMENTS

A.G. and S.M. are grateful to the UGC, New Delhi, India, for fellowships. P.D. acknowledges the CSIR of India for a fellowship. S.A. acknowledges the SERB-DST (project no. SR/S1/OC-101/2012).

■ REFERENCES

(1) (a) Fleming, C. J.; Salisbury, E. L.; Kirwan, P.; Painter, D. M.; Barnetson, R. S. *J. Am. Acad. Dermatol.* **1996**, *34*, 349−351. (b) Mainland, D. R. *Arthritis Rheum.* **1973**, *16*, 353−358. (c) Zhang, J. F.; Zhou, Y.; Yoon, J.; Kim, J. S. *Chem. Soc. Rev.* **2011**, *40*, 3416−3429.

(2) (a) Rosi, N. I.; Mirkin, C. A. *Chem. Rev.* **2005**, *105*, 1547−1562. (b) Myroshnychenko, V.; Rodriguez-Fernandez, J.; Pastoriza-Santos, I.; Funston, A. M.; Novo, C.; Mulvaney, P.; Liz-Marzan, L. M.; Garcia de Abajo, F. J. *Chem. Soc. Rev.* **2008**, *37*, 1792−1805. (c) Wang, Z.; Ma, L. *Coord. Chem. Rev.* **2009**, *253*, 1607−1618.

(3) (a) Li, Z.; Brouwer, C.; He, C. *Chem. Rev.* **2008**, *108*, 3239−3265. (b) Arcadi, A. *Chem. Rev.* **2008**, *108*, 3266−3325. (c) Gorin, D. J.; Toste, F. D. *Nature* **2007**, *446*, 395−403.

(4) (a) Goodman, C. M.; McCusker, C. D.; Yilmaz, T.; Rotello, V. M. *Bioconjugate Chem.* **2004**, *15*, 897−900. (b) Nyarko, E.; Hara, T.; Grab, D. J.; Habib, A.; Kim, Y.; Nikolskaia, O.; Fukuma, T.; Tabata, M. *Chem.-Biol. Interact.* **2004**, *148*, 19−25.

(5) Kim, C. K.; Ghosh, P.; Rotello, V. M. *Nanoscale* **2009**, *1*, 61−67.

(6) Ott, I. *Coord. Chem. Rev.* **2009**, *253*, 1670−1681.

(7) Mohamed, A. A.; Chen, J.; Bruce, A. E.; Bruce, M. R.; Bauer, J. A. K.; Hill, D. T. *Inorg. Chem.* **2003**, *42*, 2203−2205.

(8) Shaw, C. F. *Chem. Rev.* **1999**, *99*, 2589−2600.

(9) Messori, L.; Marcon, G. *Met. Ions Biol. Syst.* **2004**, *41*, 279−304.

(10) Block, W. D.; Knapp, E. L. *J. Pharm. Exp. Therap.* **1945**, *83*, 275−278.

(11) (a) Goodman, C. M.; McCusker, C. D.; Yilmaz, T.; Rotello, V. M. *Bioconjugate Chem.* **2004**, *15*, 897−900. (b) Habib, A.; Tabata, M. *J. Inorg. Biochem.* **2004**, *98*, 1696−1702.

(12) (a) Seo, H.; Jun, M. E.; Egorova, O. A.; Lee, K. H.; Kim, K. T.; Ahn, K. H. *Org. Lett.* **2012**, *14*, 5062−5065. (b) Jung Jou, M. J.; Chen, X.; Swamy, K. M. K.; Kim, H. N.; Kim, H. J.; Lee, S.; Yoon, J. *Chem. Commun.* **2009**, 7218−7220. (c) Egorova, O. A.; Seo, H.; Chatterjee, A.; Ahn, K. H. *Org. Lett.* **2010**, *12*, 401−403. (d) Yang, Y. K.; Lee, S.; Tae, J. *Org. Lett.* **2009**, *11*, 5610−5613. (e) Yuan, L.; Lin, W.; Yang, Y.; Song, J. *Chem. Commun.* **2011**, *47*, 4703−4705. (f) Song, F. L.; Ning, H. F.; She, H. Y.; Wang, J. Y.; Peng, X. J. *Sci. China: Chem.* **2014**, *57*, 1043−1047. (g) Wang, J.; Lin, W.; Yuan, L.; Song, J.; Gao, W. *Chem. Commun.* **2011**, *47*, 12506−12508. (h) Niamsa, N.; Kaewtong, C.; Srinonmuang, W.; Wanno, B.; Pulpoka, B.; Tuntulani, T. *Polym. Chem.* **2013**, *4*, 3039−3046. (i) Emrullahoglu, M.; Karakusx, E.; Üçüncü, M. *Analyst* **2013**, *138*, 3638−3641. (j) Oztas, Z.; Pamuk, M.; Algi, F. *Tetrahedron* **2013**, *69*, 2048−2051. (k) Cao, X.; Lin, W.; Ding, Y. *Chem. - Eur. J.* **2011**, *17*, 9066−9069.

(13) (a) Wang, J. B.; Wu, Q. Q.; Min, Y. Z.; Liu, Y. Z.; Song, Q. H. *Chem. Commun.* **2012**, *48*, 744−746. (b) Karakus, E.; Üçüncü, M.; Emrullahoglu, M. *Chem. Commun.* **2014**, *50*, 1119−1121. (c) Üçüncü, M.; Emrullahoğlu, M. *Chem. Commun.* **2014**, *50*, 5884−5886. (d) Park, J.; Choi, S.; Kim, T.; Kim, Y. *Analyst* **2012**, *137*, 4411−4414.

(14) (a) Seo, H.; Jun, M. E.; Ranganathan, K.; Lee, K. H.; Kim, K. T.; Lim, W.; Rhee, Y. M.; Ahn, K. H. *Org. Lett.* **2014**, *16*, 1374−1377. (b) Chinapang, P.; Ruangpornvisutia, V.; Sukwattanasinitta, M.; Rashatasakhon, P. *Dyes Pigm.* **2015**, *112*, 236−238. (c) Young Choi, J. Y.; Kim, G. H.; Guo, Z.; Lee, H. Y.; Swamy, K. M. K.; Pai, J.; Shin, S.; Shin, I.; Yoon, J. *Biosens. Bioelectron.* **2013**, *49*, 438−441.

(15) (a) Dong, M.; Wang, Y. W.; Peng, Y. *Org. Lett.* **2010**, *12*, 5310−5313. (b) Do, J. H.; Kim, H. N.; Yoon, J.; Kim, J. S.; Kim, H. J. *Org. Lett.* **2010**, *12*, 932−934. (c) Singha, S.; Kim, D.; Seo, H.; Cho, S. W.; Ahn, K. H. *Chem. Soc. Rev.* **2015**, *44*, 4367.

(16) (a) Sanz, S.; Jones, L. A.; Mohr, F.; Laguna, M. *Organometallics* **2007**, *26*, 952−957. (b) Park, J. E.; Choi, M. G.; Chang, S. K. *Inorg. Chem.* **2012**, *51*, 2880−2884.

(17) (a) Dujols, V.; Ford, F.; Czarnik, A. W. *J. Am. Chem. Soc.* **1997**, *119*, 7386−7387. (b) Yang, Y. K.; Yook, K. J.; Tae, J. *J. Am. Chem. Soc.* **2005**, *127*, 16760−16761. (c) Zhang, X.; Xiao, Y.; Qian, X. *Angew. Chem., Int. Ed.* **2008**, *47*, 8025−8029. (d) Zheng, H.; Shang, G. Q.;

DOI: 10.1021/acs.joc.5b01141
J. Org. Chem. 2015, 80, 8530−8538

Yang, S. Y.; Gao, X.; Xu, J. G. *Org. Lett.* **2008**, *10*, 2357−2360. (e) Shi, W.; Ma, H. *Chem. Commun.* **2008**, 1856−1858. (f) Zhan, X. Q.; Qian, Z. H.; Zheng, H.; Su, B. Y.; Lan, Z.; Xu, J. G. *Chem. Commun.* **2008**, 1859−1861. (g) Chen, X.; Nam, S. W.; Jou, M. J.; Kim, Y.; Kim, S. J.; Park, S.; Yoon, J. *Org. Lett.* **2008**, *10*, 5235−5238. (h) Liu, W.; Xu, L.; Zhang, H.; You, J.; Zhang, X.; Sheng, R.; Li, H.; Wu, S.; Wang, P. *Org. Biomol. Chem.* **2009**, *7*, 660−664. (i) Liu, B.; Tian, H. *Chem. Commun.* **2005**, 3156−3158. (j) Kenmoku, S.; Urano, Y.; Kojima, H.; Nagano, T. *J. Am. Chem. Soc.* **2007**, *129*, 7313−7318. (k) Chatterjee, A.; Santra, M.; Won, N.; Kim, S.; Kim, J. K.; Kim, S. B.; Ahn, K. H. *J. Am. Chem. Soc.* **2009**, *131*, 2040−2041. (l) For other references, see ref 6..

(18) (a) Kwon, J. Y.; Jang, Y. J.; Lee, Y. J.; Kim, K. M.; Seo, M. S.; Nam, W.; Yoon, J. *J. Am. Chem. Soc.* **2005**, *127*, 10107−10111. (b) Xiang, Y.; Tong, A. *Org. Lett.* **2006**, *8*, 1549−1552. (c) Wu, J. S.; Hwang, I. C.; Kim, K. S.; Kim, J. S. *Org. Lett.* **2007**, *9*, 907−910. (d) Swamy, K. W. K.; Ko, S. K.; Kwon, S. K.; Lee, H. N.; Mao, C.; Kim, J. M.; Lee, K. H.; Kim, J.; Shin, I.; Yoon, J. *Chem. Commun.* **2008**, 5915−5917. (e) Yu, M.; Shi, M.; Chen, Z.; Li, F.; Li, X.; Gao, Y.; Xu, J.; Yang, H.; Zhou, Z.; Yi, T.; Huang, C. *Chem. - Eur. J.* **2008**, *14*, 6892−6900. (f) Zhou, Z.; Yu, M.; Yang, H.; Huang, K.; Li, F.; Yi, T.; Huang, C. *Chem. Commun.* **2008**, 3387−3389. (g) Huang, K.; Yang, H.; Yu, M.; Gao, X.; Zhou, Z.; Li, F.; Yi, T.; Huang, C. *Org. Lett.* **2008**, *10*, 2557−2560. (h) Yang, H.; Zhou, Z.; Huang, K.; Yu, M.; Li, F.; Yi, T.; Huang, C. *Org. Lett.* **2007**, *9*, 4729−4732. (i) Zhang, M.; Li, M.; Gao, Y.; Yu, M.; Li, F.; Zhu, M.; Zhang, J.; Yi, T.; Huang, C. *Tetrahedron Lett.* **2007**, *48*, 3709−3712. (j) Kou, S.; Lee, H. N.; Noort, D. V.; Swamy, K. M. K.; Kim, S. H.; Soh, J. H.; Lee, K.; Nam, S.; Yoon, J.; Park, S. *Angew. Chem., Int. Ed.* **2008**, *47*, 872−876. (k) Soh, J. H.; Swamy, K. M. K.; Kim, S. K.; Kim, S.; Lee, S. H.; Yoon, J. *Tetrahedron Lett.* **2007**, *48*, 5966−5969. (l) Zhou, Y.; Fang, W.; Kim, Y.; Kim, S.; Yoon, J. *Org. Lett.* **2009**, *11*, 4442−4445. (m) For other references, see ref 6..

(19) (a) Sahana, A.; Banerjee, A.; Lohar, S.; Sarkar, B.; Mukhopadhyay, S. K.; Das, D. *Inorg. Chem.* **2013**, *52*, 3627−3633. (b) Albers, A. E.; Okreglak, V. S.; Chang, J. C. *J. Am. Chem. Soc.* **2006**, *128*, 9640−9641.

(20) Geißler, D.; Stufler, S.; Löhmannsröben, H. G.; Hildebrandt, N. *J. Am. Chem. Soc.* **2013**, *135*, 1102−1109.

(21) Ho, T. L. *Chem. Rev.* **1975**, *75*, 1−20.

(22) (a) Mei, Q.; Wang, L.; Tian, B.; Yan, F.; Zhang, B.; Huang, W.; Tong, B. *New J. Chem.* **2012**, *36*, 1879−1883. (b) Park, S.; Kim, W.; Swamy, K. M. K.; Lee, H. Y.; Jung, J. Y.; Kim, G.; Kim, Y.; Kim, S. J.; Yoon, J. *Dyes Pigm.* **2013**, *99*, 323−328.

(23) (a) Saha, S.; Mahato, P.; Reddy G, U.; Suresh, E.; Chakrabarty, A.; Baidya, M.; Ghosh, S. K.; Das, A. *Inorg. Chem.* **2012**, *51*, 336−345. (b) Han, Z. X.; Zhang, X. B.; Li, Z.; Mao, G. J.; Jin, Z.; Shen, G. L.; Yu, R. Q.; Wu, X. Y. *Anal. Lett.* **2010**, *43*, 2751−2761.

(24) Benesi, H. A.; Hildebrand, J. H. *J. Am. Chem. Soc.* **1949**, *71*, 2703−2707.

(25) Frisch, M. J.; Trucks, G. W.; Schlegel, H. B.; Scuseria, G. E.; Robb, M. A.; Cheeseman, J. R., et al. *Gaussian 09, revision A.01*; Gaussian, Inc., Wallingford, CT, 2009.

(26) Lakowicz, X. J. R. *Principles of Fluorescence Spectroscopy*; University of Maryland School of Medicine: Baltimore, MD, USA, 2006.

(27) Achremowicz, L. *Synth. Commun.* **1996**, *26*, 1681−1684.

(28) Zhang, X.; Shiraishi, Y.; Hirai, T. *Org. Lett.* **2007**, *9*, 5039−5042.

(29) (a) Wei, N.; Murthy, N. N.; Chen, Q.; Zubieta, J.; Karlin'J, K. D. *Inorg. Chem.* **1994**, *33*, 1953−1965. (b) Zahn, S.; Das, D.; Canary, J. W. *Inorg. Chem.* **2006**, *45*, 6056−6063.

DOI: 10.1021/acs.joc.5b01141
J. Org. Chem. 2015, 80, 8530−8538